J Mol Model (2014) 20:2457
DOI 10.1007/s00894-014-2457-4

ORIGINAL PAPER

Theoretical study on the tautomerization of 1,5-diaminotetrazole (DAT)

Piao He · Jian-Guo Zhang · Li-Na Feng · Kun Wang · Tong-Lai Zhang · Shao-Wen Zhang

Received: 1 April 2014 / Accepted: 1 September 2014 / Published online: 21 September 2014

Abstract The tautomerization pathways and kinetics of 1,5-diaminotetrazole (DAT) have been investigated by means of second-order Møller-Plesset perturbation theory (MP2) and coupled-cluster theory, with single and double excitations including perturbative corrections for triple excitations (CCSD(T)). Five possible tautomers, namely 4-hydro-1-amino-5-imino-tetrazole (a), 2,5-diamino-tetrazole (b), 1,5-diamino-tetrazole (c), 2-hydro-1-imino-5-amino-tetrazole (d), and 2,4-dihydro-1,5-diimino-tetrazole (e) were identified. The structures of the reactants, transition states, and products along with the tautomerism pathways were optimized by the MP2 method using the 6-311G** basis set, and the energies were refined using CCSD(T)/6-311G**. The minimum-energy path (MEP) information for DAT was obtained at the CCSD(T)/6-311G**//MP2/6-311G** level of theory. Therein, reaction 2 (c → b) is an amino-shift reaction, while reaction 1 (c → a), reaction 3 (c → d), reaction 4 (a → e), and reaction 5 (d → e) are reactions of hydrogen-shift tautomerization. The calculated results show that 2,5-diaminotetrazole (b) with the minimum energy (taking c as a standard) among five tautomers, is the energetically preferred tautomer of DAT in the gas phase. In addition, the energy barrier of reaction 2 is 71.65 kcal·mol^{-1} in the gas phase, while reaction 1 takes place more easily with an activation barrier of 61.53 kcal·mol^{-1} also as compared to 63.71 kcal·mol^{-1} in reaction 3. Moreover, the tautomerization of reaction 4 requires the largest energy barrier of 83.29 kcal·mol^{-1}, which is obviously bigger than reaction 5 with a value of 73.78 kcal·mol^{-1}. Thus, the hydrogen-shift of c to a is the easiest transformation, while the tautomerization of a to e is the hardest one. Again, the rate constants of tautomerization have been obtained by TST, TST/Eckart, CVT, CVT/SCT, and CVT/ZCT methods in the range 200-2500 K, and analysis indicated that variational effects are small over the whole temperature range, while tunneling effects are significant in the lower temperature range.

Keywords 1,5-Diamino-tetrazole · Hydrogen Shift · Kinetics · Tautomerism · Tunneling Effect

P. He · J.-G. Zhang (✉) · L.-N. Feng · K. Wang · T.-L. Zhang
State Key Laboratory of Explosion Science and Technology, Beijing Institute of Technology, Beijing, People's Republic of China 100081
e-mail: zjgbit@bit.edu.cn

L.-N. Feng
Shanxi Fenxi Heavy Industry Co., Ltd, Taiyuan, People's Republic of China 030027

K. Wang
Department of Chemistry, Inorganic Chemistry Laboratory, University of Oxford, South Parks Road, Oxford OX1 3QR, UK

S.-W. Zhang
School of Chemistry, Beijing Institute of technology, Beijing, People's Republic of China 100081

Introduction

Tetrazoles are important high-energy self-organized combustion compounds, burning at the expense of their own components without any oxidizer [1]. Tetrazole derivatives are characterized by extreme properties among azoles, such as the highest N–H-acidity, the lowest basicity, and the presence of several "pyridine-like" nitrogen atoms [2]. These features along with biological activity of tetrazoles and their high nitrogen content and positive enthalpies of formation have made these substances and their complexes interesting for many different branches of science, pharmaceutical [3–5], and material chemistry including gas-generating and energetic

materials [6–13], ferromagnets [14], and other materials for molecular electronics [15–17]. 1,5-Diaminotetrazole (DAT), as a fascinating component in the construction of high energy density materials because of its unique structure and remarkable properties, has attracted considerable attention [7, 18–25].

There has been considerable and continuing interest in the co-existence of tautomers of tetrazoles. A lot of experimental and theoretical studies have been devoted to the tautomerism and protonation of tetrazole [26, 27]. Results show that the temperature-dependent tautomeric amino-imino and prototropic transformations are important preliminary steps in reactions of 5-aminotetrazole (ATZ) [28]. We have studied the tautomerism of ATZ, and found that six possible tautomers could exist in theory, namely 1*H*,4*H*-5-imino-tetrazole, 1-*H*-5-amino-tetrazole, 2-*H*-5-amino-tetrazole, 1*H*,2*H*-5-imino-tetrazole, the mesoionic form, and 2*H*,4*H*-5-imino-tetrazole. In principle, DAT may coexist in amino and imino tautomeric forms in the solid state and probably also in the melted [29].

To the best of our knowledge, few studies have been concerned with 1,5-diaminotetrazole, and the present investigation was undertaken to study the mechanism and kinetics of the tautomerization of DAT in the same way as for ATZ. This paper focuses on the tautomers and intramolecular hydrogen shift of DAT (Fig. 1) and their kinetics in the gas phase. The aims of our study are to determine the stability of the tautomers and the mechanism of these tautomerization reactions, and obtain more kinetic information for the title reactions, including the rate constants over a wide temperature range. Specifically, we have focused on the importance of the tunneling effect. With a clearer knowledge of the existing forms, some new complexes may be obtained, and the results may prove useful in rationalizing certain phenomena and explaining some experimental data, such as the infrared spectrum, the various products of decomposition, and so on.

Computational methods

All calculations were carried out with the Gaussian 03 program [30]. The optimized geometries and harmonic vibrational frequencies of all stationary points (the reactants, products, and transition states) were optimized with restricted second-order Møller−Plesset perturbation theory using the 6-311G** basis set. To yield more reliable enthalpies and barrier heights, we performed single-point energy calculations for the stationary points by the CCSD(T) method with the 6-311G** basis set. The intrinsic reaction coordinate (IRC)[31], and the minimum-energy path (MEP), were obtained at the MP2/6-311G** level to confirm that whether the transition states really connect with minima along the reaction path. The MEP was calculated in mass-weighted Cartesian coordinates with a gradient step size of 0.02 $(amu)^{1/2}$ bohr. The energy derivatives, including gradients and Hessians at geometries of some selected points (17 points on each side) along the MEP, were calculated at the same level. The single-point energy calculations for the points along the MEP were then refined to establish the potential curve at the CCSD(T)/6-311G** level of theory.

All of the rate constants reported herein were evaluated over a wide temperature range from 200 to 2500 K using conventional, non-variational transition-state theory (TST) [32], TST rate constant calculations with the Eckart tunneling correction (TST/Eckart) [33], canonical variational transition-state theory (CVT)[34–36], canonical variational transition-state theory with small curvature tunneling correction (CVT/SCT) [37, 38], and canonical variational transition-state theory with zero-curvature tunneling correction (CVT/ZCT) [39, 40] by means of the Vklab program package [41] and the POLYRATE 8.2 program [42].

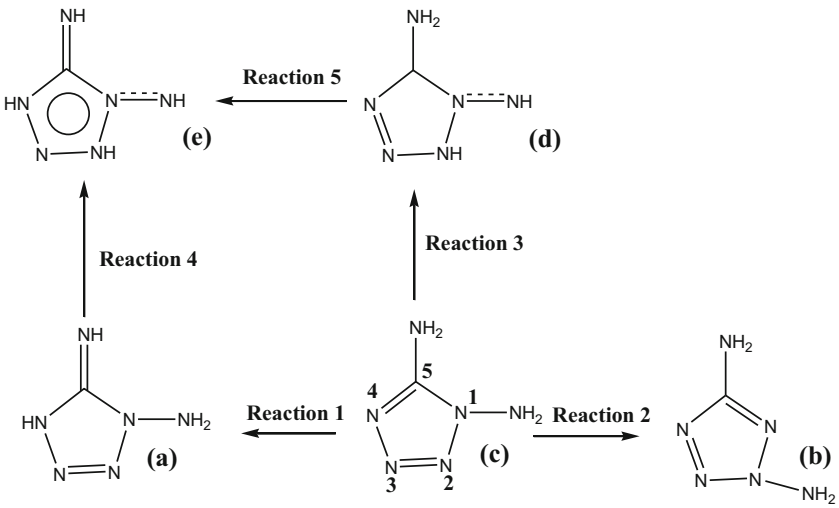

Fig. 1 The tautomers and reactions of the tautomerism of DAT using the MP2/6-311G**

Table 1 The optimized geometries of tautomers of DAT and the transition states at MP2/6-311G**

	a	*TSc-a*	*c*	*TSc-b*	*b*	*TSc-d*	*d*	*TSa-e*	*e*	*TSd-e*
R(1,4)	1.279	1.327	1.375	1.378	1.383	1.376	1.395	1.274	1.282	1.329
R(1,7)	1.019	1.013	1.012	1.010	1.011	1.014	1.014		1.018	1.017
R(1,8)		1.488	1.010	1.011	1.011	1.012	1.014	1.018		1.506
R(2,3)	1.291	1.308	1.312	1.317	1.336	1.333	1.359	1.326	1.364	1.388
R(2,5)	1.362	1.381	1.351	1.462	1.322	1.329	1.354	1.332	1.383	1.407
R(3,6)	1.354	1.350	1.364	1.342	1.333	1.345	1.324	1.359	1.362	1.366
R(4,5)	1.397	1.351	1.352	1.347	1.349	1.350	1.388	1.420	1.425	1.390
R(4,6)	1.384	1.345	1.323	1.344	1.348	1.344	1.340	1.397	1.378	1.338
R(5,9)	1.379	1.657	1.388			1.389	1.297	1.389	1.303	1.638
R(6,8)	1.007	1.276				1.602		1.024	1.010	1.276
R(9,10)	1.015	1.016	1.016	1.025	1.017	1.023		1.620	1.025	1.025
R(9,11)	1.015		1.016	1.024	1.017		1.024			
R(5,9)		1.385		1.952						1.298
R(2,9)				1.903	1.389					
A(4,1,7)	107.8	118.5	112.8	113.3	112.5	111.7	111.1	109.1	109.9	116.4
A(3,2,5)	107.3	107.4		108.5		111.3		114.3	113.2	114.0
A(2,3,6)	107.7	107.6		109.9	104.8	105.8	105.6	101.2	99.9	100.0
A(1,4,5)	134.0	147.5	123.2	123.3	122.9	123.7	118.5	133.8	130.9	141.8
A(1,4,6)	127.5	107.4	128.5	123.9	123.6	127.9	131.5	126.7	127.7	109.4
A(5,4,6)	98.5	104.3	108.2	112.8	113.5	108.3	110.0	99.4	101.4	107.8
A(2,5,4)	112.9	109.4	109.3	101.7	99.9	105.8	102.2	108.4	106.0	101.6
A(2,5,9)	123.5	123.0	125.0			106.1	122.0	104.4	122.3	130.9
A(4,5,9)	123.5	127.4	125.7	107.5		143.6		133.3	131.7	126.6
A(3,6,4)	113.6	111.0	105.8	106.7	106.0	108.6	109.4	115.7	117.4	114.6
A(5,9,10)	108.9	107.8	107.3	78.6				106.0	104.4	106.7
A(5,9,11)	108.9	107.9	108.0	113.2		105.8				
A(10,9,11)	109.1	108.3	108.1	103.6	108.3	121.0		124.4		
A(4,1,8)			111.9	112.1	111.2	111.2	111.5			

Table 2 Harmonic frequencies (cm^{-1}) and intensities ($km \cdot mol^{-1}$), for the reactants, products, and transition states at MP2/6-311G**

Species	*Harmonic frequencies*	*ZPE*
a	106(9),192(14),297(1),423(134),501(36),649(24),697(21),708(4),743(44),925(49),1002(72),1091(107),1106(19),1219(9), 1336(114),1351(2),1433(3),1487(8),1695(9),1801(431),3533(4),3558(17),3630(14),3715(122)	50.90
TSc-a	1852i(738),191(6),257(39),308(10),497(190),575(21),600(22),693(4),715(8),859(3),964(73),971(65),1034(70),1097(13), 1172(81),1237(42),1258(47),1363(3),1389(17),1505(52),1673(64),1748(290),2084(83),3531(6),3626(32),3627(17)	47.45
c	211(6),255(32),269(27),308(5),346(13),480(14),649(92),691(33),710(40),754(118),791(22),976(37),1035(43),1107(18),1158(26), 1193(1),1271(33),1359(7),1369(16),1563(30),1600(10),1666(115),1718(130),3529(10),3595(38),3624(21),3713(47)	51.38
TSc-b	915i(59),112(33),120(8),256(5),306(28),387(1),546(35),578(35),685(127),735(9),753(120),890(85),930(1),1008(2),1028(58), 1089(26),1142(6),1153(5),1195(8),1440(10),1547(62),1566(96),1658(176),3445(10),3543(10),3601(43),3715(39)	47.90
b	112(55),197(14),259(38),321(5),351(2),493(10),644(12),667(29),694(121),779(124),816(37),1033(118),1039(22),1097(1), 1135(16),1229(20),1277(7),1421(10),1469(9),1522(46),1574(93),1660(190),1672(33),3516(11),3600(32),3623(25),3712(33)	51.34
TSc-d	1584i(687),219(17),239(9),297(10),325(12),537(35),571(45),669(64),697(14),713(21),789(231),833(21),1020(9),1068(112), 1108(8),1168(30),1223(14),1255(64),1364(1),1419(26),1496(3),1598(42),1669(219),2243(171),3481(2),3568(34),3687(50)	47.54
e	176(1),225(10),317(32),372(6),430(2),489(18),516(195),592(115),604(46),618(16),700(13),886(63),1053(123),1122(14), 1203(88),1269(9),1320(53),1360(42),1457(35),1517(67),1776(363),1975(2073),3462(1),3563(9),3605(99),3685(111)	50.16
TSa-e	1499i(55),172(15),214(0),327(5),511(59),579(121),594(235),656(32),687(49),724(9),755(45),843(56),948(19),1030(145), 1073(248),1126(33),1231(43),1277(21),1349(42),1396(37),1428(6),1462(23),1779(434),2290(112),3458(6),3574(21),3655(115)	47.38
d	145(28),226(3),257(14),300(3),407(108),516(48),594(84),640(11),693(12),714(9),796(33),817(57),982(24),1079(26),1189(31), 1215(7),1229(35),1292(54),1407(2),1486(20),1561(20),1650(41),1686(95),3481(28),3560(11),3646(24),3652(122)	50.36
TSd-e	1815i(313),214(19),259(3),301(17),393(20),489(115),542(10),594(79),616(116),648(86),710(9),840(37),920(21),1005(163), 1101(51),1115(25),1184(30),1192(67),1354(89),1405(33),1486(75),1666(322),1928(572),2101(73),3469(16),3573(31),3584(63)	46.73

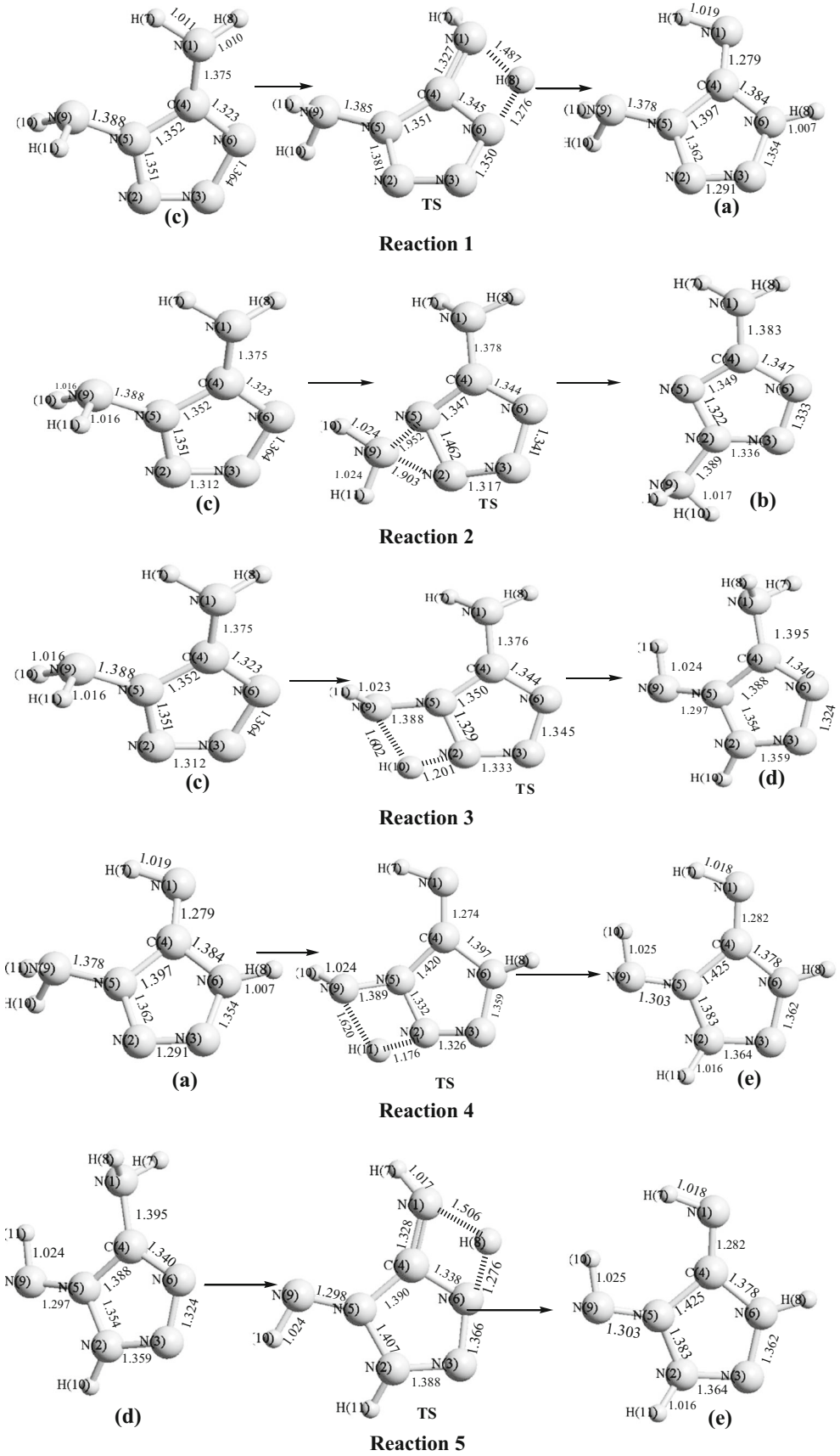

Fig. 2 The mechanism of the tautomeric equilibrium and hydrogen shifts of DAT

Results and discussion

The geometries and vibrational frequencies

We considered five tautomers of DAT in this study for comparison. The optimized structures for the reactants, products, and transition states consisting of the main bond parameters at the MP2/6-311G** level of theory, are given in Table 1. The experimental length of C = N bond is 1.273 Å in $H_2C = NH$, and the bond length of C-N is 1.474 Å in CH_3NH_2 [43]. The distances of N-N in H-N = N-H and H_2N-NH_2 are 1.252 and 1.449 Å, respectively [44].

For tautomers a, c, d, and e, nearly all of the skeletal bonds are calculated to lie between isolated single and double bonds, except for the C_4-N_1 bond of a, the C_4-N_5 and N_3-N_2 bonds of c, and the C_4-N_1 and N_5-N_9 bonds of e, which are close to double bonds. The atoms of a and c are nearly in a plane with deviations of less than 0.5°, except for the hydrogen atoms of amino. The rings of d and e show a greater deviation from planarity and there is significant repulsion between the hydrogen atoms on N_1 and N_9 in e. For tautomer b, nearly all of the skeletal bonds are calculated to lie between isolated single and double bonds, and the atoms are not coplanar, showing greater deviations from planarity of 5°.

The skeletal bond lengths calculated for both b and c (Table 1) lie between those of isolated single and double bonds. The results clearly suggest that the lone pairs of electrons at N_2 in b and at N_5 in c are delocalized in planar five-center 6π electron aromatic systems, indicating that the molecules are aromatic, which may be the reason for the greater stability of these tautomers. 2*H*-5-amino-tetrazole has previously been suggested as a stable tautomer of ATZ, and our calculations show that 2,5-diamino-tetrazole (b) is also the most stable tautomer of DAT in theory.

Both the optimization and the frequency calculations were successfully completed for all of the reactants, products, and transition states of the above mentioned five reactions at the MP2/6-311G** level. Reactants and products were observed as local minima with positive vibrational frequencies. Only one imaginary frequency was found for each transition state, and the transition states of all five reactions were first-order saddle points in the potential barriers of the reaction paths. The infrared spectra of all five tautomers and the transition states of the tautomeric equilibria of the hydrogen shift are summarized in Table 2. The mechanisms of the tautomerization reactions are shown in Fig. 2. $TS_{c\text{-}a}$, $TS_{c\text{-}b}$, $TS_{c\text{-}d}$, $TS_{a\text{-}e}$, and $TS_{d\text{-}e}$ denote the transition states of reactions 1, 2, 3, 4, and 5, respectively, and normal-mode analysis revealed that they have only one imaginary frequency corresponding to exchange of the hydrogen atoms. The imaginary frequencies of $TS_{c\text{-}a}$, $TS_{c\text{-}b}$, $TS_{c\text{-}d}$, $TS_{a\text{-}e}$, and $TS_{d\text{-}e}$ are 1852*i* cm^{-1}, 915*i* cm^{-1}, 1584*i* cm^{-1}, 1499*i* cm^{-1}, and 1815*i* cm^{-1}, respectively. Because a, b, c, d, and e were calculated to have similar IR spectra, it may not be straightforward to use IR spectroscopy to differentiate between these tautomers.

Energy barriers to tautomerism

The minimum-energy paths were obtained using the intrinsic reaction coordinate (IRC) theory at the MP2/6-311G** level of theory, and the potential energy profiles were further refined using CCSD(T)/6-311G**. Table 3 gives the reaction enthalpies (ΔH^0_{298K}), the reaction energies (ΔE), the classical potential barriers (V_{MEP}), the ground-state adiabatic energy curve (V_a^G), which is defined by the refined energies calculated using CCSD(T)/6-311G** with zero-point energies at the MP2/6-311G** level (V_{MEP} + ZEP).

These data show that, although less stable than tautomers b and c, tautomers a, d, and e are good candidates for experimental observation and worthy topics for future research. We can also conclude from Table 3 that all of these reactions are endothermic processes. These reactions may play an important role in both the atmosphere and in combustion systems of DAT. The order of V_a^G in the forward direction is reaction 4 > reaction 5 > reaction 2 > reaction 3 > reaction 1. The value of V_a^G in reaction 1 and reaction 3 are similar and that of V_a^G in reaction 2 is larger. Thus the result indicates that hydrogen shifts such as c → a and c → d are easier than c → b as amino shifts. A schematic representation of the tautomers and transition states for DAT is shown in Fig. 3.

It can be seen that a, b, and c are relatively more stable than d and e. As a result, the value of V_a^G in reaction 4 and reaction 5 may be larger, and the low V_a^G of the reverse reactions in reactions 3, 4, and 5 also show that d and e are very unstable. For the reverse direction, the order of V_a^G is reaction 2 > reaction 1 > reaction 3 > reaction 4 > reaction 5. Finally, all of the results point to the fact that reactions 3, 4, and 5 are irreversible exothermic processes. All of these reactions need a suitable source of energy or an appropriate catalyst to proceed.

Figure 4 shows the adiabatic ground-state potential energy curves (V_a^G) and the classical potential barriers (V_{MEP}) of the reactions. As can be seen, the curve of reaction 2 is smoother, in accordance with the fact that the imaginary frequency of the transition state of this reaction is smaller, which indicates the

Table 3 The energy parameters (kcal·mol^{-1}) of each tautomerism reaction of DAT

	ΔH^0_{298k}	ΔE	V_{MEP}	V_a^G	V_a^G (*Reverse*)
Reaction 1	50.22	12.38	65.46	61.53	49.15
Reaction 2	77.91	-0.109	75.29	71.65	71.76
Reaction 3	64.87	39.909	67.55	63.71	23.80
Reaction 4	44.63	68.53	86.80	83.29	14.75
Reaction 5	23.29	61.12	77.41	73.78	12.66

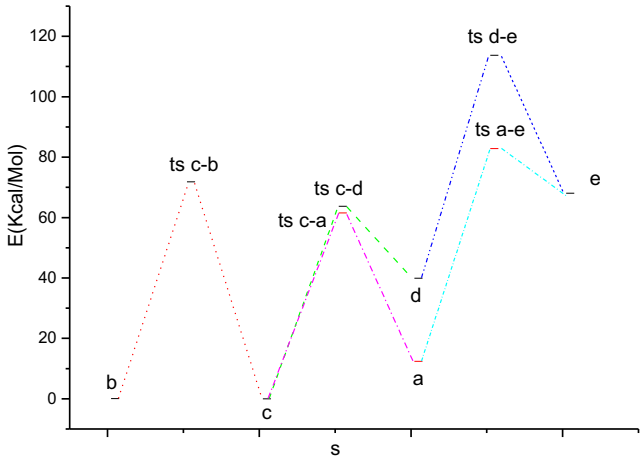

Fig. 3 Schematic representation of tautomers and transition states of DAT

tunneling effect of reaction 2 is smaller. Apart from reaction 2 as an amino-shift reaction, the other four reactions are quite similar because they are all hydrogen-shift reactions. In general, the transition states of hydrogen-shift reactions have higher imaginary frequencies and more cuspidaler curves with a greater tunneling effect.

In summary, the tautomers a and d are expected to be most easily derived from c experimentally. While b is the most stable, but is difficult to interchange with c. Again e is the least stable, while the probability of this reaction from c to e occurring is low because of the largest V_a^G of the transformation. All of the $V_{MEP}(s)$ and $V_a^G(s)$ curves are similar in shape and their maxima are located at the same position (s=0), which implies that the variational effect in calculating the rate constants of the reactions will be small to some extent.

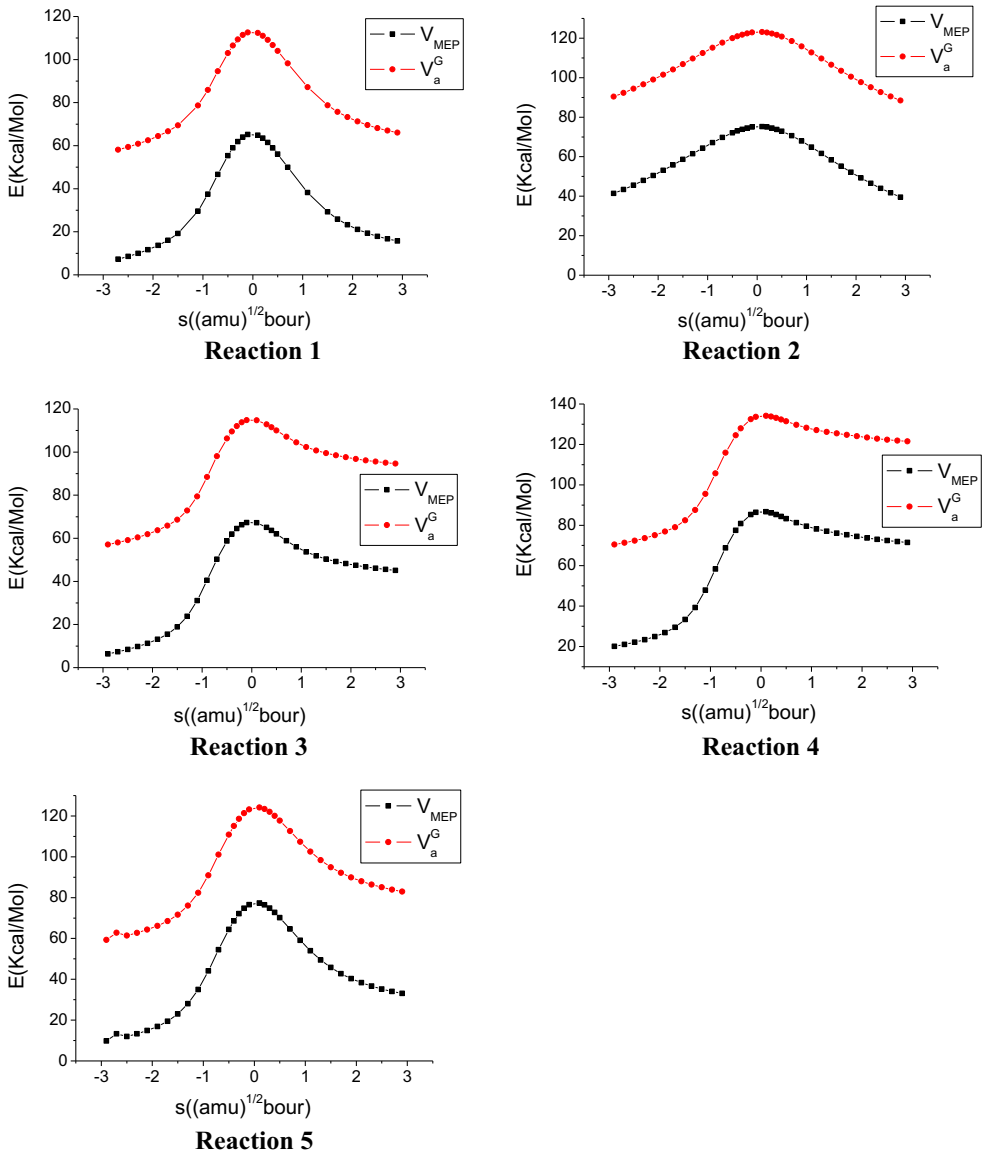

Fig. 4 The adiabatic ground-state potential energy curves (V_a^G) and the classical potential barriers (V_{MEP}) of the reactions as a function of s (amu)$^{1/2}$ bohr at the MP2/6-311G** level of theory

Rate constants of tautomerization

Thermal rate constants are essential in modeling the tautomerization of DAT. Furthermore, accurate rate constants are increasingly needed for process simulations and are also necessary for quantifying the competing reactions. The interpolated variational transition-state theory, based on the minimum-energy path calculated at the MP2/6-311G** level of theory was used to calculate the reaction rates, and this approach was improved by interpolated corrections of barrier height at the CCSD(T)/6-311G** level. Overall reaction rate constants were calculated by TST and CVT theory, which corresponds to classical reaction-coordinate, and by TST with Eckart correction. Since the tunneling cannot be underestimated for reactions such as hydrogen exchange, dehydrogenation, and hydrogen migration, etc., a correction for tunneling was estimated using the ZCT and SCT approximations. The rate constants at several temperatures are depicted in Fig. 5 and detailed results are shown in Table 4.

The variational effect, that is, the ratio of rate constants between the variational CVT and conventional TST, was considered as well. For these five reactions, throughout the studied temperature range, the CVT curves are nearly superimposable on the TST curves, and the data calculated using these two methods show only slight disparity, so there is little variational effect on the title reactions.

For reaction 1, the discrepancies in the rate constants calculated using the TST, TST/Eckart, CVT/SCT, and CVT/ZCT methods are significantly large only at lower temperatures (200 K < T < 500 K). With increasing temperature, the deviations become small. It can easily be concluded that tunneling has a distinct effect on this reaction at low temperatures but has little effect at high temperatures. At lower temperatures, the larger discrepancies occur due to the higher values of E_a and the pre-exponential factor in the TST and CVT equations. At the higher temperatures, the smaller discrepancies appear due to the lack of a temperature in the pre-exponential factor. However, at 300 K, the rate constant

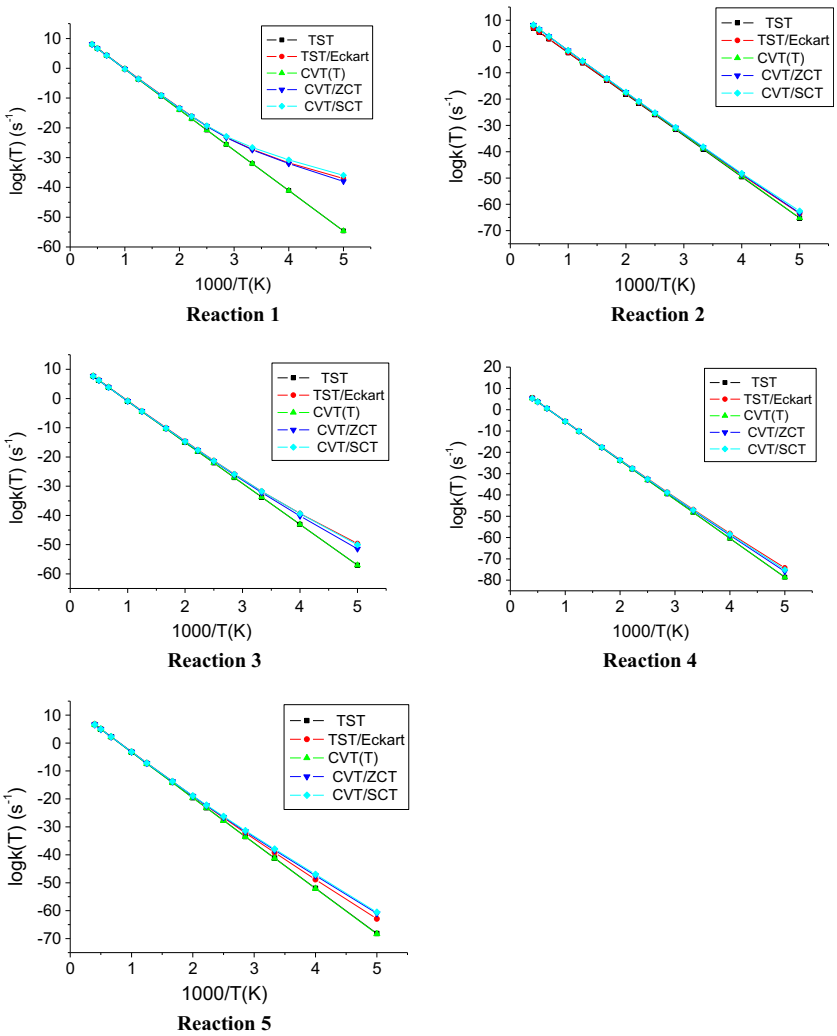

Fig. 5 Arrhenius plot of the rate constants calculated at the TST, TST/Eckart, CVT, CVT/SCT, and CVT/ZCT levels of theory. The rate constants are calculated based on the interpolated MEP at the MP2/6-311G** level of theory

Table 4 Rate constants (in s^{-1}) at several temperatures

T(K)	TST	TST/Eckart	CVT	CVT/ZCT	CVT/SCT	
Reaction 1	200	2.56E-55	1.00E-37	2.49E-55	1.05E-38	1.19E-36
	300	9.47E-33	5.51E-28	9.28E-33	4.12E-28	2.61E-27
	400	1.92E-21	4.97E-20	1.89E-21	3.51E-20	4.85E-20
	500	1.20E-14	6.14E-14	1.18E-14	4.34E-14	4.61E-14
	800	2.04E-04	3.84E-04	2.01E-04	2.76E-04	2.78E-04
	1000	5.45E-01	8.54E-01	5.39E-01	6.31E-01	6.33E-01
	1500	2.15E+04	2.79E+04	2.13E+04	2.20E+04	2.20E+04
	2000	4.46E+06	5.34E+06	4.41E+06	4.40E+06	4.40E+06
	2500	1.11E+08	1.28E+08	1.10E+08	1.08E+08	1.09E+08
Reaction 2	200	5.44E-66	2.91E-64	6.75E-66	4.72E-64	2.78E-63
	300	8.53E-40	2.49E-39	1.60E-39	5.20E-39	7.41E-39
	400	1.09E-26	2.03E-26	2.72E-26	5.09E-26	6.05E-26
	500	7.98E-19	1.24E-18	2.50E-18	3.75E-18	4.17E-18
	800	5.05E-07	6.37E-07	2.52E-06	3.01E-06	3.14E-06
	1000	4.28E-03	5.11E-03	2.66E-02	3.01E-02	3.09E-02
	1500	7.01E+02	7.82E+02	6.36E+03	6.81E+03	6.89E+03
	2000	2.68E+05	2.90E+05	3.23E+06	3.38E+06	3.40E+06
	2500	9.11E+06	9.70E+06	1.37E+08	1.42E+08	1.42E+08
Reaction 3	200	8.92E-58	2.26E-50	9.03E-58	3.73E-52	9.37E-51
	300	1.91E-34	1.73E-32	1.92E-34	6.35E-33	1.73E-32
	400	9.19E-23	5.83E-22	9.24E-23	3.61E-22	4.90E-22
	500	9.66E-16	2.93E-15	9.71E-16	1.97E-15	2.27E-15
	800	3.57E-05	5.85E-05	3.58E-05	4.26E-05	4.45E-05
	1000	1.24E-01	1.77E-01	1.24E-01	1.34E-01	1.38E-01
	1500	6.94E+03	8.57E+03	6.94E+03	6.93E+03	7.01E+03
	2000	1.71E+06	1.98E+06	1.71E+06	1.67E+06	1.68E+06
	2500	4.73E+07	5.31E+07	4.73E+07	4.61E+07	4.62E+07
Reaction 4	200	2.43E-79	6.31E-75	2.13E-79	1.22E-76	7.92E-76
	300	6.13E-49	1.43E-47	5.59E-49	4.32E-48	8.38E-48
	400	9.99E-34	4.54E-33	9.29E-34	2.50E-33	3.23E-33
	500	1.37E-24	3.58E-24	1.29E-24	2.33E-24	2.68E-24
	800	7.46E-11	1.17E-10	7.18E-11	8.90E-11	9.31E-11
	1000	2.94E-06	4.08E-06	2.85E-06	3.26E-06	3.35E-06
	1500	4.19E+00	5.09E+00	4.08E+00	4.32E+00	4.37E+00
	2000	5.20E+03	5.97E+03	5.07E+03	5.22E+03	5.25E+03
	2500	3.79E+05	4.23E+05	1.99E+05	2.01E+05	2.02E+05
Reaction 5	200	6.92E-69	1.20E-63	4.97E-69	1.14E-61	3.05E-61
	300	6.48E-42	5.99E-40	5.21E-42	4.81E-39	1.15E-38
	400	2.09E-28	1.87E-27	1.77E-28	2.98E-27	5.21E-27
	500	2.74E-20	1.05E-19	2.41E-20	1.03E-19	1.36E-19
	800	4.47E-08	8.05E-08	4.14E-08	6.61E-08	7.12E-08
	1000	5.48E-04	8.36E-04	5.15E-04	6.81E-04	7.12E-04
	1500	1.64E+02	2.10E+02	1.57E+02	1.71E+02	1.75E+02
	2000	9.29E+04	1.11E+05	8.99E+04	9.14E+04	9.23E+04
	2500	4.24E+06	4.85E+06	4.12E+06	4.05E+06	4.08E+06

calculated using the CVT/SCT method is 2.61×10^{-27}, indicating that the thermal reaction is far too slow to play a role in atmospheric chemistry.

For reactions 3 and 5, the rate constants calculated using the TST/Eckart, CVT/SCT, and CVT/ZCT methods show only slight deviations compared to those calculated by the

TST and CVT methods. It can be concluded that tunneling has smaller effects on these reactions at low temperatures than on reaction 1. For reaction 4, a smaller deviation compared to the values calculated by the TST method was found at low temperatures (200 K < T < 500 K), indicating that the effect of tunneling on this reaction is smallest among reactions 3, 4, and 5. In any case, our calculations indicate that the tunneling effect plays an important role in the hydrogen-shift tautomerization reactions of DAT than previously believed.

While for reaction 2 as an amino-shift reaction, the rate constants calculated by means of the TST, TST/Eckart, CVT, CVT/SCT, and CVT/ZCT methods are also almost identical at high temperatures (T > 500 K). At low temperatures (200 K < T < 500 K), the rate constants calculated by means of the TST/Eckart, CVT/SCT, and CVT/ZCT methods are almost identical, and there is little deviation compared to the values calculated by the TST and CVT methods. It can be concluded that tunneling has little effect on this reaction at low temperatures.

As can be seen in Table 4, the rate constant of reaction 4 is the highest, followed by those of reaction 5, reaction 2, reaction 3, and reaction 1. This order is in agreement with the adiabatic barriers (83.29 kcal·mol^{-1} (4), 73.78 kcal·mol^{-1} (5), 71.65 kcal·mol^{-1} (2), 63.71 kcal·mol^{-1} (3), and 61.53 kcal·mol^{-1} (1)). All of the rate constants increase rapidly with increasing temperature, especially in the lower temperature range.

Therefore, for the reactions under consideration, the variational effect is small over the whole temperature range. For the four hydrogen-shift reactions, V_a^G is larger, and the tunneling effect is smaller. In addition, the CVT/SCT rate constants in the range 200-2500 K were fitted by a three-parameter method ($k=AT^n\exp(-E_a/RT)$) for the five reactions as follows:

$$k(T) = 2.262 \times 10^{-58} \times T^{20.42} \times e^{-\left(1.25\times10^4/T\right)}\ \mathrm{s}^{-1}$$
$$k(T) = 6.941 \times 10^{3} \times T^{3.07} \times e^{-\left(3.40\times10^4/T\right)}\ \mathrm{s}^{-1}$$
$$k(T) = 1.405 \times 10^{-13} \times T^{7.50} \times e^{-\left(2.544\times10^4/T\right)}\ \mathrm{s}^{-1}.$$
$$k(T) = 2.500 \times 10^{1} \times T^{3.24} \times e^{-\left(3.88\times10^4/T\right)}\ \mathrm{s}^{-1}$$
$$k(T) = 8.418 \times 10^{-12} \times T^{6.87} \times e^{-\left(3.02\times10^4/T\right)}\ \mathrm{s}^{-1}$$

Conclusions

The tautomerization reactions of DAT have been studied in detail. The geometries and frequencies of all stationary points, corresponding to the reactants, products and transition states, as well as the MEP, have been calculated at the MP2/6-311G** level of theory, and single-point energies have been calculated by CCSD(T)/6-311G**. Again the thermal rate constants for the reactions were evaluated using the TST, TST/Eckart, CVT, CVT/SCT, and CVT/ZCT methods in the temperature range 200-2500 K. For the tautomers of DAT, calculations predicted a reasonable cyclic structure. In the gas phase, 2,5-diaminotetrazole (b) is predicted to be the dominant form, followed by 1,5-diaminotetrazole (c). The stabilities of b and c can be ascribed to their aromatic character with delocalization of the lone pair on the saturated nitrogen atom into the five-membered ring to form a 6π electron aromatic system. As a result, the hydrogen-shift of c to a is the easiest transformation, while the tautomerization of a to e is the hardest one. Moreover, the transition-state theory calculations have indicated that tunneling plays a modest role in these hydrogen-transfer reactions, such as reactions 1, 3, and 5, while there is a smaller tunneling effect on reactions 2 and 4.

Finally, it is expected that the present theoretical study may be useful for estimating the kinetics of the reactions over a wide temperature range, for which no experimental data are available.

Acknowledgments The authors would like to thank Professor D. G. Truhlar for providing the POLYRATE 8.2 program. The project was supported by the NSAF Foundation (No. 10776002) of National Natural Science Foundation of China and Chinese Academy of Engineering Physics.

References

1. Lesnikovich A, Sviridov V, Printsev G et al (1986) A new type of self-organization in combustion. Nature 323:706–707
2. Gaponik PN, Voitekhovich SV, Lyakhov AS et al (2005) Crystal structure and physical properties of the new 2D polymeric compound bis (1, 5-diaminotetrazole) dichlorocopper (II). Inorg Chim Acta 8: 2549–2557
3. Bekhit AA, El-Sayed OA, Al-Allaf AKT et al (2004) Synthesis, characterization and cytotoxicity evaluation of some new platinum(II) complexes of tetrazolo[1,5-a]quinolines. Eur J Med Chem 6:499–505
4. Herr RJ (2002) 5-Substituted-1H-tetrazoles as carboxylic acid isosteres: medicinal chemistry and synthetic methods. Bioorg Med Chem 11:3379–3393
5. Pais GCG, Zhang X, Marchand C et al (2002) Structure activity of 3-aryl-1,3-diketo-containing compounds as HIV-1 integrase inhibitors1. J Med Chem 15:3184–3194
6. Piekiel N, Zachariah MR (2012) Decomposition of aminotetrazole based energetic materials under high heating rate conditions. J Phys Chem A 6:1519–1526
7. Tao G-H, Guo Y, Parrish DA et al (2010) Energetic 1,5-diamino-4H-tetrazolium nitro-substituted azolates. J Mater Chem 15:2999–3005
8. Tao G-H, Guo Y, Joo Y-H et al (2008) Energetic nitrogen-rich salts and ionic liquids: 5-aminotetrazole (AT) as a weak acid. J Mater Chem 45:5524–5530
9. Zhang Q, Zhang J, Parrish DA et al (2013) Energetic N-trinitroethyl-substituted mono-, di-, and triaminotetrazoles. Chem Eur J 33: 11000–11006
10. Zhang Q, Shreeve JNM (2013) Growing catenated nitrogen atom chains. Angew Chem Int Ed 34:8792–8794
11. Tang Y, Yang H, Cheng G (2013) Recent advanced strategies for extending the nitrogen chain in the synthesis of high nitrogen compounds. Synlett 17:2183–2187

12. Fischer D, Klapoetke TM, Piercey DG et al (2013) Synthesis of 5-aminotetrazole-1 N-oxide and its azo derivative: a key step in the development of new energetic materials. Chem Eur J 14:4602–4613
13. Hollo B, Jaso V, Leovac VM et al (2013) Synthesis, structure and thermokinetic studies on perchlorate salts of metal complexes containing a formamidine-type ligand. J Coord Chem 3:453–463
14. Stassen AF, Kooijman H, Spek AL et al (2002) Strongly isolated ferromagnetic layers in poly-trans-μ-dichloro- and poly-trans-μ-dibromobis(1-(2-chloroethyl)-tetrazole-N4)copper(II) complexes. Inorg Chem 24:6468–6473
15. Stassen AF, Driessen WL, Haasnoot JG et al (2003) Structure and magnetic properties of the weak ferromagnet bis(1-(2-chloroethyl)-tetrazole)bis(nitrato)copper(II). Inorg Chim Acta 57:61
16. Stassen AF, Roubeau O, Ferrero Gramage I et al (2001) Physical properties of the spin-crossover compound hexakis(1-methyltetrazole-N4)iron(II) triflate, steady state and relaxation studies, X-ray structure of the isomorphic Ni(II) compound. Polyhedron 11–14:1699–1707
17. Roubeau O, Stassen AF, Gramage IF et al (2001) Surprising features in old and new [Fe(alkyl-tetrazole)6] spin-crossover systems. Polyhedron 11–14:1709–1716
18. Cui Y, Zhang J, Zhang T et al (2008) Synthesis, structural investigation, thermal decomposition mechanism and sensitivity properties of an energetic compound Cd(DAT)(6) (ClO(4))(2) (DAT = 1,5-diaminotetrazole). J Hazard Mater 1:45–50
19. Joo YH, Twamley B, Shreeve JM (2009) Carbonyl and oxalyl bridged bis(1,5-diaminotetrazole)-based energetic salts. Chem Eur J 36:9097–9104
20. Joo Y-H, Twamley B, Garg S et al (2008) Energetic nitrogen-rich derivatives of 1,5-diaminotetrazole. Angew Chem Int Ed 33:6236–6239
21. Klapoetke TM, Martin FA, Stierstorfer J (2012) N-bound primary nitramines based on 1,5-diaminotetrazole. Chem Eur J 5:1487–1501
22. Shang J, Zhang J, Cui Y et al (2010) Synthesis, crystal structure, and properties of an energetic compound Zn(1,5-diaminotetrazole)(6)(ClO4)(2). Acta Chim Sinica 3:233–238
23. Sinditskii VP, Egorshev VY, Dutova TY et al (2011) Combustion of derivatives of 1,5-diaminotetrazole. Explo Shock Waves 1:36–44
24. Wu B-D, Li F-G, Zhang T-L et al (2013) Preparation, crystal structure, and thermal decomposition of the four-coordinated zinc compound based on 1,5-diaminotetrazole. Z Anorg Und Allg Chem 7:1248–1253
25. Gao H, Shreeve JNM (2011) Azole-based energetic salts. Chem Rev 11:7377–7436
26. Jimenez V, Alderete JB (2006) Complete basis set calculations on the tautomerism and protonation of triazoles and tetrazole. J Mol Struct 775:1–7
27. Chen ZX, Xiao JM, Chin YN (1999) Studies on heats of formation for tetrazole derivatives with density functional theory. J Phys Chem A 103:8062–8066
28. Levchik SV, Ivashkevich OA, Balabanovich AI et al (1992) Thermal decomposition of 5-aminotetrazoles. Thermochim Acta 207:115
29. Levchik SV, Balabanovich AI, Ivashkevich OA et al (1993) The thermal decomposition of aminotetrazoles. Part 2. 1-Methyl-5-aminotetrzole and 1,5-diaminotetrazole. Thermochim Acta 225:53–65
30. Frisch MJ, Trucks GW, Schlegel HB, et al (2003) Gaussian 03, revision A1. Gaussian Inc, Pittsburgh, PA
31. Gonzalez C, Schlegel HB (1989) IRC. J Chem Phys 90:2154
32. Truhlar DG, Isaacson AD, Garrett BC (1985) Theory of Chemical reaction dynamics, vol. 4 [M]. CRC, Boca Raton
33. Truong NT, Truhlar DG (1990) TST/Eckart. J Chem Phys 93:1761
34. Miller WH (1979) CVT. J Am Chem Soc 101:6810
35. Truhlar DG, Garrett BC (1984) CVT. Annu Rev Phys Chem 35:159
36. Truong NT (1994) CVT. J Chem Phys 100:8014
37. Liu YP, Lynch GC, Troung TN et al (1993) CVT/SCT. J Am Chem Soc 115:2408
38. Truhlar DG, Isaacson AD, Garrett BC (1982) CVT/SCT. J Phys Chem 85:2252
39. Garrett BC, Truhlar DG, Grev RS et al (1980) ZCT. J Phys Chem 84:1730
40. Truhlar DG, Isaacson AD, Skodje RT et al (1982) ZCT. J Phys Chem 86:2252
41. Zhang SW, Truong TN (2001) VKLab version 1.0 [M]. University of Utah
42. Chuang YY, Corchado JC, Fast PL, et al (1999) POLYRATE, Program vision 8.2 [M]. Minneapolis
43. Zhang L P, Tu Y R (1980) Foundation of organic chemistry (theory and application) (trans) [M]. Higher Education Press, Beijing
44. Harmony MD, Laurie VW, Kuczkowski RL et al (1979) Molecular structures of gas-phase polyatomic molecules determined by spectroscopic methods. J Phys Chern Ref Data 3:619–722